

# Staying connected: assessing the capacity of landscapes to retain biodiversity in a changing climate

Tom David Harwood (✉ [tom.harwood@csiro.au](mailto:tom.harwood@csiro.au))

CSIRO: Commonwealth Scientific and Industrial Research Organisation <https://orcid.org/0000-0002-3855-5306>

**Jamie Love**

NSW Department of Planning Industry and Environment

**Michael Drielsma**

NSW Department of Planning Industry and Environment

**Clare Brandon**

CSIRO: Commonwealth Scientific and Industrial Research Organisation

**Simon Ferrier**

CSIRO: Commonwealth Scientific and Industrial Research Organisation

---

## Research Article

**Keywords:** Spatial resilience, biodiversity, climate change, habitat condition, habitat connectivity

**Posted Date:** February 25th, 2022

**DOI:** <https://doi.org/10.21203/rs.3.rs-1360584/v1>

**License:**  This work is licensed under a Creative Commons Attribution 4.0 International License.

[Read Full License](#)

---

1 **Staying connected: assessing the capacity of landscapes to retain**  
2 **biodiversity in a changing climate**

3

4 **Tom Harwood<sup>a</sup>, Jamie Love<sup>c</sup>, Michael Drielsma<sup>c</sup>, Clare Brandon<sup>b</sup> and Simon Ferrier<sup>a</sup>**

5 <sup>a</sup>Commonwealth Scientific and Industrial Research Organisation, Canberra, ACT, Australia

6 <sup>b</sup>Commonwealth Scientific and Industrial Research Organisation, Brisbane, Queensland, Australia

7 <sup>c</sup>New South Wales, Department of Planning, Industry and Environment, Armidale, NSW, Australia

8

9

10

11

12

13

14

15

16

17

18

19

20

21

22

23

24

25

26 **Keywords**

27 Spatial resilience; biodiversity; climate change; habitat condition; habitat connectivity

28

29 **Acknowledgements**

30 This work was funded by the NSW Environmental Trust.

## 31 **Abstract**

32

33 *Context* Management for positive biodiversity outcomes under a changing climate requires a  
34 shift of perspective relative to traditional conservation. Here we develop a repeatable  
35 indicator for measuring the capacity of landscapes to retain biodiversity under a range of  
36 plausible climate futures, as a function of the condition and spatial configuration of native  
37 habitat.

38

39 *Methods* The Spatial Resilience Index extends an existing approach to assessing the potential  
40 for biodiversity associated with any location in a region to access suitable habitat in the  
41 surrounding landscape under climate change, incorporating multiple dispersal rates integrated  
42 over time and an optimised spatial structure. Derivation of the indicator is demonstrated for  
43 an Australian case study, covering the entire State of New South Wales, drawing on existing  
44 spatial datasets and models.

45

46 *Results* Mapping of the Spatial Resilience Index across New South Wales suggests that  
47 different regions, and locations within these regions, vary markedly in their expected capacity  
48 to retain biodiversity, depending on the direct rate of climate change, the degree of climatic  
49 buffering (or reduction of climate velocity) afforded by landscape heterogeneity, and the  
50 degree of anthropogenic impacts on the connectedness of habitat in the landscape. The  
51 developed approach accounts for the interplay between these processes by treating them  
52 within a unified framework.

53

54 *Conclusions* The index highlights areas which can potentially benefit from adaptive  
55 management (e.g. habitat restoration) to enhance capacity to retain biodiversity under climate  
56 change, and offers an objective means of monitoring any resulting change in this capacity  
57 over time.

58

## 59 **Introduction**

60

61 Growing awareness of the impacts that climate change is already having, and is expected to continue  
62 having, on the distribution and viability of species and ecological communities has motivated  
63 considerable reappraisal of the fundamental goals and strategies of nature conservation over recent  
64 years (Prober et al. 2019). A common theme emerging from this thinking is the concept of “managing  
65 for change” (Stein et al. 2013; van Kerkhoff et al. 2019). From a biodiversity conservation  
66 perspective, managing for change entails a shift from the traditional focus on securing and  
67 maintaining species or communities where they occur at present, towards a strategy which embraces  
68 the possibility that the distributions of at least some species will need to shift under climate change,  
69 thereby altering the composition of present-day communities. The fundamental goal of biodiversity  
70 conservation implicit in this way of thinking is about ensuring persistence of collective biological  
71 diversity, i.e. “gamma diversity”, within some relatively large spatial extent (Mokany et al. 2013) –  
72 e.g. a whole landscape, a country, a continent, or ultimately the entire planet. Change in the  
73 distribution of species, and in the composition of communities at local scales, is therefore viewed as  
74 being essential to enabling retention of gamma diversity, e.g. total number of species persisting,  
75 within the whole region of interest. If couched in terms of ecological resilience theory (Holling 1973;  
76 Quinlan et al. 2016), this local-scale biological reorganisation is what underpins the capacity of the  
77 broader system to retain its essential structure (in this case retention of gamma diversity) in the face of  
78 a major, yet highly uncertain, stressor (in this case climate change).

79 Efforts to enhance the capacity of a landscape or region to retain biodiversity under climate change  
80 focus most commonly on actions aimed at either: 1) preventing future loss in the condition of  
81 relatively intact native vegetation through habitat protection; or 2) improving the condition of  
82 relatively degraded areas through various forms of habitat restoration. Most practitioners involved in  
83 such efforts are, however, acutely aware that biodiversity persistence under climate change is likely to  
84 be a function not just of the total amount of habitat protected and/or restored in a landscape, but also  
85 of the spatial location and configuration of that habitat. If the spatial distribution of fundamental  
86 climatic niches of species are shifting then the persistence of these species will depend, at least in part,

87 on the availability of habitat within areas of suitable climate under future, not just present, climatic  
88 conditions (Hannah et al. 2007). For at least some species the ability to disperse to climatically  
89 suitable areas of habitat into the future will also depend on the degree to which present and future  
90 habitats are connected spatially (Keeley et al. 2018). The role that habitat connectedness across space  
91 and time plays in enabling persistence of biodiversity under climate change therefore constitutes an  
92 important facet of the ‘spatial resilience’ of natural systems (Cumming 2011).

93 Effective consideration of these factors continues to pose significant challenges for quantitative  
94 science-based analyses aiming to inform large-scaled habitat protection and restoration efforts  
95 (Donaldson et al. 2017; Gillson et al. 2013; Jones et al. 2016). To help appreciate the nature of these  
96 challenges it is worth first distinguishing between two broad types of question typically addressed by  
97 such analyses. The first type of question relates to the expected capacity of a given system, as a whole  
98 (e.g. an entire landscape or region), to retain biodiversity in the face of ongoing climate change given  
99 the present condition and spatial configuration of habitat across that system. Assessing capacity at this  
100 whole-system level can help in characterising the overall need for action to protect and/or restore  
101 habitat. Repeated application of such an assessment also offers a means of monitoring the extent to  
102 which a system’s expected capacity to retain biodiversity has improved or declined over time as a  
103 function of observed changes in habitat condition or configuration, including as a result of any  
104 implemented management. The second type of question relates to the prioritisation of individual  
105 management actions. Assuming that the decision has already been made to invest in a program of  
106 habitat protection or restoration within a given landscape or region, then this is the challenge of  
107 deciding precisely where best to direct this effort spatially within the system concerned.

108 Approaches to addressing these two types of question are often developed and applied in isolation  
109 from each other. For example, while techniques for mapping potential climate refugia (e.g.  
110 Baumgartner et al. 2018), or significant pathways of habitat connection (e.g. Nunez et al. 2013), can  
111 play a valuable role in informing spatial prioritisation of habitat protection or restoration, they rarely  
112 provide an adequate foundation for assessing and monitoring the capacity of an entire system to retain  
113 biodiversity under climate change. Effectively coupling the prioritisation of individual actions and

114 system-level monitoring requires an integrated approach to addressing these activities within an  
115 adaptive policy or management framework. A relatively straightforward strategy for achieving such  
116 integration is to view, and perform, spatial prioritisation of actions within a broader landscape as a  
117 logical extension of the analytical approach used to assess the state of that landscape at a whole-  
118 system level (Ferrier and Drielsma 2010). This involves predicting the marginal gain in the overall  
119 state of the system – in this case, the system’s capacity to retain biodiversity in the face of climate  
120 change – expected to result from implementation of a given action, i.e. habitat protection or  
121 restoration at a particular location in the landscape.

122 Here we describe a new indicator – the Spatial Resilience Index – for assessing system-level capacity  
123 to retain biodiversity in the face of climate change as a function of the condition and spatial  
124 configuration of habitat across the entire Australian State of New South Wales (NSW), covering an  
125 area of 801,150 km<sup>2</sup>. This work builds on a solid foundation of biodiversity-related spatial data, and  
126 associated models, already established by previous studies across NSW including existing indicators  
127 of habitat condition Love et al. (2020) and ecosystem persistence Drielsma et al. (2020) delivered  
128 under the NSW biodiversity indicator program. Also of direct relevance and value to the current work,  
129 are the data and models generated by Drielsma et al.’s (2017) analysis of potential impacts of  
130 plausible climate futures on biodiversity, and prioritisation of revegetation actions to ameliorate these  
131 impacts.

132 Our approach to developing the new indicator is based on, and extends, that already employed in  
133 deriving an indicator assessing capacity to retain biodiversity in the face of climate change at global  
134 scale – the Bioclimatic Ecosystem Resilience Index, BERI (Ferrier *et al.*, 2020a). This particular  
135 approach offers an alternative to, and effectively occupies the middle ground between, the two major  
136 analytical paradigms which have dominated most other efforts to address this general challenge over  
137 recent years. The first of these paradigms focuses on modelling shifts in the distribution of individual  
138 species as a spatially explicit function of projected changes in climate, employing an extensive array  
139 of correlative and mechanistic modelling techniques (Urban et al. 2016). While advances continue to  
140 be made in extending these techniques to account for complicating factors such as population

141 dynamics, evolutionary adaptation, and species interactions, the species-specific data and knowledge  
142 needed to undertake such modelling is rarely available for more than a small proportion of all species.  
143 This has motivated many workers to explore the second of these two major paradigms, which focuses  
144 exclusively on analysing spatiotemporal patterns and dynamics of abiotic environmental variables  
145 alone, without any direct use of biological data or explicit modelling of biological responses (Carroll  
146 et al. 2017). Prominent examples of this paradigm include analyses of climate velocity – i.e. the speed  
147 at which hypothetical organisms associated with a given location would need to move across the  
148 landscape to track projected shifts in climate (Brito-Morales et al. 2018) – and adaptation strategies  
149 based on “conserving nature’s stage” (Beier et al. 2015) – i.e. ensuring that retained areas of natural  
150 habitat encompass high levels of diversity in, and steep gradients of, climate and other relevant abiotic  
151 variables (e.g. soils).

152 In common with this second paradigm, the approach we employ here makes no attempt to explicitly  
153 model responses of individual species to climate change. However, unlike other applications of the  
154 paradigm, our approach works with environmental variables (including climate variables) which have  
155 been non-linearly scaled to better reflect the observed effect that changes in these variables have on  
156 the species composition of ecological communities. This is achieved by applying generalised  
157 dissimilarity modelling, GDM (Ferrier et al. 2007) to best-available occurrence records for large  
158 numbers of species to transform multidimensional environmental space such that distances within this  
159 transformed space correlate as closely as possible with observed levels of turnover in species  
160 composition between locations under present-day climatic conditions. Space-for-time substitution can  
161 then be used to predict the level of compositional turnover expected between a location under present  
162 conditions and either itself, or another location, under any future climate scenario (Blois et al. 2013;  
163 Ferrier et al. 2012; Fitzpatrick et al. 2011).

164 The existing global-scale BERI indicator (Ferrier *et al.*, 2020a) combines GDM-based modelling of  
165 compositional turnover with cost-benefit assessment of habitat connectivity (Drielsma et al. 2007a) to  
166 estimate the connectedness of a given focal grid-cell to areas of supporting natural habitat in the  
167 surrounding landscape which, under a plausible range of climate futures, are predicted to support an

168 assemblage of species similar to that of the focal cell under present climatic conditions. This indicator  
169 provides an effective means of assessing capacity to retain biodiversity from the perspective of each-  
170 and-every individual cell in a region of interest, thereby allowing variation in this capacity to be  
171 mapped across that region. Here we significantly extend this existing analytical capability to derive a  
172 truly system-level indicator of the capacity of an entire region (in this case the state of NSW) to retain  
173 biodiversity in the face of climate change. This is achieved by making further use of fitted GDM-  
174 based models to integrate consideration of spatial variation in species composition, i.e. ‘beta  
175 diversity’, into the estimation of the region’s collective capacity to retain gamma diversity.

176 We demonstrate the utility of this extended approach for whole-system monitoring by generating  
177 results for the new indicator across NSW, employing high resolution habitat-condition mapping and  
178 GDM modelling of vascular-plant compositional turnover, while additionally accounting for plausible  
179 variation in future climate trajectories and in maximum velocities of biological redistribution expected  
180 for different plant-dispersal modes. Although beyond the scope of this initial study, it is also intended  
181 that the indicator will, in the future, provide a foundation for prioritising actions aimed at enhancing  
182 the capacity of this system to retain biodiversity under climate change.

## 183 **Methods**

184

185

### 186 **Overview**

187

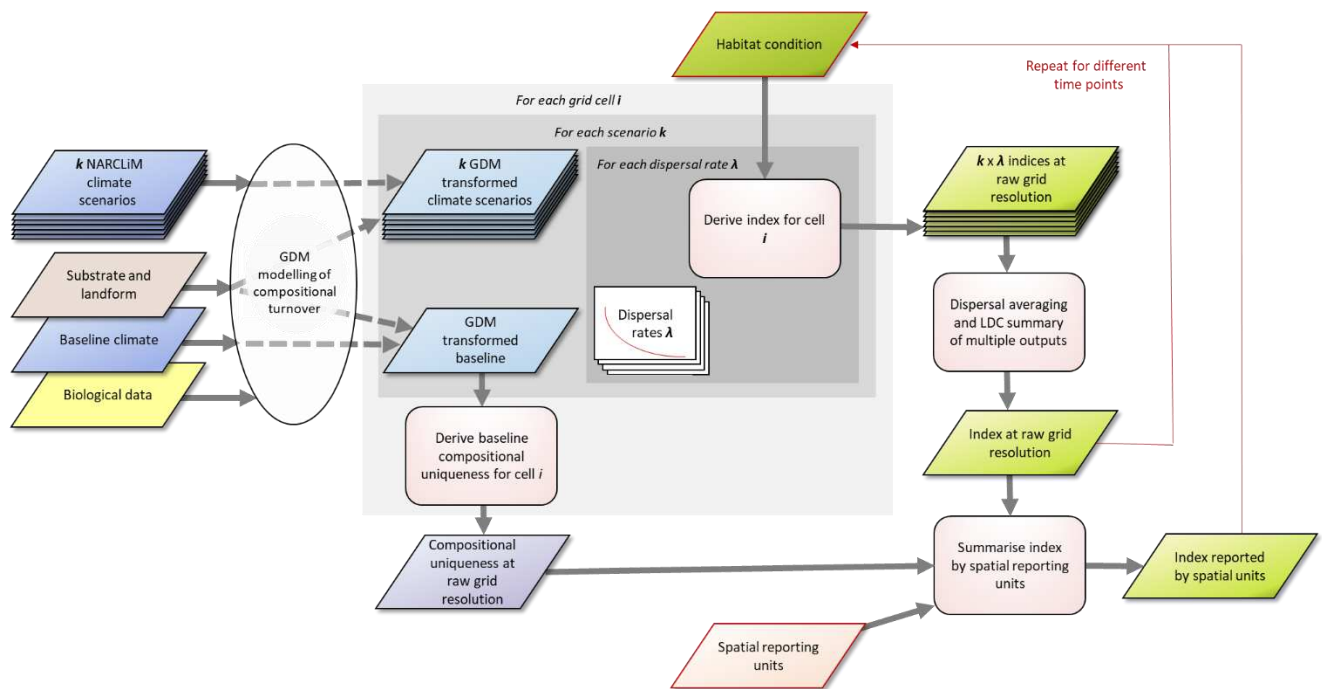
188 The Spatial Resilience Index, operationalised here for reporting across NSW, builds on the cost-  
189 benefit approach to assessing habitat connectivity originally described by Drielsma *et al.* (Drielsma et  
190 al. 2007b) and applied in a climate change context at global scale in the BERI indicator (Ferrier et al.  
191 2020). The application within NSW further builds on existing biodiversity and environmental data  
192 layers and models already in use across the State, at 9 arc-second (250m) resolution. Climate  
193 scenarios were drawn from the NSW/ACT Regional Climate Modelling project (NARCLiM) (Evans et  
194 al., 2014) domain, which provides extensive buffering beyond the State borders as required in any  
195 study of ecological responses to climate change. Modelling of current and future patterns of turnover  
196 in species composition across space and time was based on GDM models previously fitted within the  
197 NARCLiM domain (M. Drielsma et al., 2015) and used to assess ecosystem persistence (M. Drielsma  
198 et al., 2020) under the NSW biodiversity indicator program (OEH & CSIRO, 2019). A habitat  
199 condition surface for this same domain was drawn from the Biodiversity Impacts and Adaptation  
200 Project (BIAP) undertaken by M. J. Drielsma et al. (2017), and updated within NSW to include more  
201 recent modelling of ecological condition (Love et al., 2020) also published as part of the NSW  
202 biodiversity indicator program.

203 The complete workflow for derivation of the Spatial Resilience Index is illustrated in Figure 1. Firstly,  
204 a GDM model is fitted to current climate, static landform and substrate descriptors and aggregated  
205 biological survey data. The model predicts the level of dissimilarity (or conversely similarity) in  
206 species composition expected between any pair of grid-cells if those cells were still covered by intact  
207 native habitat. This model of present-day patterns of compositional similarity between cells is then  
208 used to project, through space-for-time substitution, changes in these patterns expected in the future as  
209 a function of different climate scenarios. This is achieved by using the GDM-based nonlinear  
210 transformations of climate variables, fitted to the present-day data, to transform both the present-day  
211 and future climate grids.

212 A grid of current habitat condition is then used to derive the Spatial Resilience Index for each  
213 individual cell. This involves estimating the connectivity of that cell to all cells in the surrounding  
214 landscape which are predicted (based on the GDM modelling) to be able to support a similar  
215 composition of species, under a given climate scenario, to that currently supported by the cell of  
216 interest. This analysis is repeated for a representative set of climate scenarios, and a plausible range  
217 of median dispersal distances for the biological group concerned (i.e. vascular plants in the case of  
218 this study). The resulting estimates of the total amount of compositionally-similar habitat which is  
219 well connected to the cell of interest are then averaged across these analyses. The cellwise Spatial  
220 Resilience Index is derived by expressing this average as a proportion of the maximum possible value  
221 obtained if the entire landscape were covered by intact habitat, and climatic conditions are fixed at  
222 their current level.

223 Scaling up the cellwise calculations described above, to thereby assess the capacity of whole regions  
224 to retain biodiversity under climate change, requires consideration of spatial variation in species  
225 composition (i.e. beta diversity) both within and between these regions. To help enable this  
226 assessment, the present-day GDM model is further used to estimate the compositional uniqueness of  
227 each cell within the NARCLiM domain.

228 We now describe in greater depth each of these steps in deriving the Spatial Resilience Index.



229

230 **Fig. 1:** Workflow for the calculation of the Spatial Resilience Index. .

231

232

233 **Generalised Dissimilarity Modelling**

234

235 A Generalised Dissimilarity Model of compositional turnover in vascular plants (Drielsma et al. 2015)

236 was used to map the distribution of cells predicted to have a similar ecological environment in the

237 future to that currently associated with a given focal cell. The GDM scales the similarity in

238 environment between two locations in terms of the predicted Sørensen-index similarity in their

239 species composition. The model was fitted within the NARCLiM climate domain (full extent shown

240 in Fig. S2) which includes all of NSW, the Australian Capital Territory, and Victoria, and is further

241 buffered into Queensland and South Australia in order to adequately represent climate change

242 processes in NSW.

243 Two categories of environmental variables were used in the modelling, those that change over time as

244 a function of projected climate change, and landform and substrate descriptors which are in this case

245 assumed to be constant over the time period. NARCLiM provides a full suite of 20-year climate

246 scenarios for a baseline ‘present’ period 1990-2009, and two future periods, of which we selected one,  
 247 2060-2079 for this analysis. The dataset covers four Global Climate Models (GCMs) spanning a range  
 248 of possible futures: CSIRO mk3.0 (warm, dry); MIROC 3.2 (warm, wet); MPI ECHAM 5 (hot, dry);  
 249 and CCCMA3 (hot, wet). For each of these GCMs, three Regional Climate Models (RCMs) are used  
 250 to downscale the data to a 250m grid for the entire domain. A single socio-economic scenario, SRES  
 251 A2 was modelled in NARClIM. This scenario remains consistent with the world’s current trajectory  
 252 and has equivalent forcing to Representative Concentration Pathway 8.5. Summary climate metrics  
 253 were derived using ANUCLIM 6.1 (Hutchinson and Xu 2015).

254 A suite of environmental layers were provided as candidate predictor variables for the GDM model  
 255 described below, and Table S1 lists the 25 variables included in the final model and their sources.

256 Subsequent spatio-temporal analysis and projection of the fitted GDM model is achieved by  
 257 transformation of the environmental layers for each climate scenario. The predicted pairwise  
 258 similarity ( $s$ ) between any two grid cells ( $i, j$ ) separated by space and/or time can then be calculated as  
 259 a function of the sum across all layers of the absolute pairwise difference between grid cells ( $|x_i - x_j|$ )  
 260 within each transformed layer ( $x$ ) following (Ferrier et al. 2007) as

$$261 \quad s_{ij} = e^{-\sum_{x=1}^{x=25} |x_i - x_j|}$$

262 For any grid cell ( $i$ ), it is also possible to calculate a continuous measure of the relative area of similar  
 263 ecological environments in an intact pre-industrial landscape as the sum of pairwise similarities  
 264 ( $\sum_{j=1}^{j=N_{all}} s_{ij}$ ) to all ( $N_{all}$ ) other cells ( $j$ ). The inverse of this sum provides a measure of the original  
 265 compositional uniqueness of each cell (Supplementary Figure S2a). Those ecological environments  
 266 that are relatively unique, such as the high alpine areas will have a lower  $\sum s_{ij}$  than more common  
 267 environments. This surface was generated for the baseline climate and was then saved for subsequent  
 268 use in summarising the Spatial Resilience Index for regional reporting units.

269

270 **Habitat Condition**

271

272 Habitat condition is here used to describe the cellwise intactness of native vegetation relative to its  
273 pre-industrial state. This is represented as an index from 0 (totally transformed) to 1 (totally intact) for  
274 each grid-cell and is the key test variable being assessed by the indicator. At the resolution of an  
275 individual cell, within which we assume homogeneity, habitat condition can be viewed as a proxy for  
276 local system resilience (*sensu* Cumming (2011)). The impact of changes in landscape-scale habitat  
277 condition, through ongoing degradation or restoration are reflected in the Spatial Resilience Index.  
278 However, it is worth noting that the assessment of condition beyond the site scale is challenging, and  
279 that issues such as inaccuracies or resolution issues in input data and the requirement to average  
280 condition across all states within grid cells will always be limiting factors. Here we used a condition  
281 surface previously generated for reporting in NSW. This surface synthesises land cover, land use,  
282 fractional cover dynamics and other landscape features (Love et al, 2020) (Drielsma et al. 2015) and  
283 represents a habitat-condition baseline (*h*) centred on 2013. Key assumptions underpinning the  
284 extrapolation of the surface beyond NSW (following Drielsma *et al.*, 2015) are that locations which  
285 have a similar structural type and annual variability will have similar condition under similar  
286 management, that particular land-use or management practices have the same consequences in the  
287 same vegetation type, and that these relationships (calibrated for NSW) are constant across the study  
288 area. Whilst these areas beyond NSW have reduced resolution, they are used only as a buffer region to  
289 avoid edge effects in the analysis.

290

## 291 Calculation of the Spatial Resilience Index per grid cell

292

293 The Spatial Resilience Index was calculated for the full set of NARCLiM futures, taking into account  
294 a range of effective dispersal distances. The cellwise calculation of the index for each dispersal  
295 distance was based on the Ferrier et al. (2020) extensions of the Drielsma et al. (2007b) cost-benefit  
296 approach, thereby enabling assessment of habitat connectivity in a climate-change context. Our  
297 application of this approach employs a new formalised geometric structure to maximise the rigour  
298 with which habitat connectivity is assessed within the neighbourhood around each focal cell.

299 *Radial geometric structure*

300

301 In common with other spatial analyses, the geometric configuration of spatial units employed directly  
302 affects the results. The Spatial Resilience Index is calculated using a radial grid of connected  
303 “segments” – defined here as the intersection between sectors and radial bands – increasing in size  
304 with distance from the focal cell. Habitat condition is then averaged across all 250m cells falling  
305 within each segment. Drielsma et al. (2007b) do not define a particular geometry in their original  
306 description of the cost-benefit approach, but show a figure with irregular ‘petals’. More recent  
307 iterations such as Drielsma et al. (2017) have defined a radial structure with approximate doubling of  
308 petal area in concentric rings. The BERI index for tropical forests (Ferrier et al. 2020), working at  
309 1km grid-resolution globally, uses a grid split into 8 radial sectors (N, NE, E, SE, S, SW, W, NW),  
310 with concentric circles at radii of 2, 5, 10, 25, 50, 100, 200, 300, 400, and 500km selecting by the cell  
311 centres. Whilst these regular approaches seem straightforward, and are well behaved at band widths of  
312 greater than 5 or 6 cells, their behaviour breaks down close to the focal cell (where connectivity is  
313 critical) as the size of the radial segments approaches that of the underlying raster’s resolution and the  
314 cartesian and polar-coordinate systems interact. Here there is a tendency for adjacent segments to  
315 change drastically in shape and orientation, making it difficult to treat them as equivalent units, and  
316 with some configurations resulting in non-concentric geometries. Since connectivity in the immediate  
317 vicinity of the test cell is critical, a more reliable spatial definition is required.

318 In order to formalise the geometric structure relative to the raster cell size, we established some  
319 simple guidelines. Firstly, the 8 radial sectors centred on the cardinal and ordinal directions from  
320 BERI were used, distributing segments equally in all directions. Secondly, the principle (Drielsma et  
321 al. 2017) of a regular stepwise (near doubling) increase in area in concentric bands was set as a target.  
322 Lastly, visual inspection of the geometric structure close to the test cell was carried out to examine the  
323 extent to which each radial band of segments conformed to the shape of the radial segments at greater  
324 radii. An exploratory environment was set up, and different approaches were iteratively tested against  
325 these criteria. Whilst there are only a limited number of possible geometries close to the focal cell, a  
326 generalised formulation that is equally applicable at all scales was defined relative to the cartesian

327 grid. Bands were defined (Supplementary Table S2) by including all cells with cell centres within a  
 328 specified radius and specific radii were generated up to a maximum radius of 200 grid  
 329 cells.

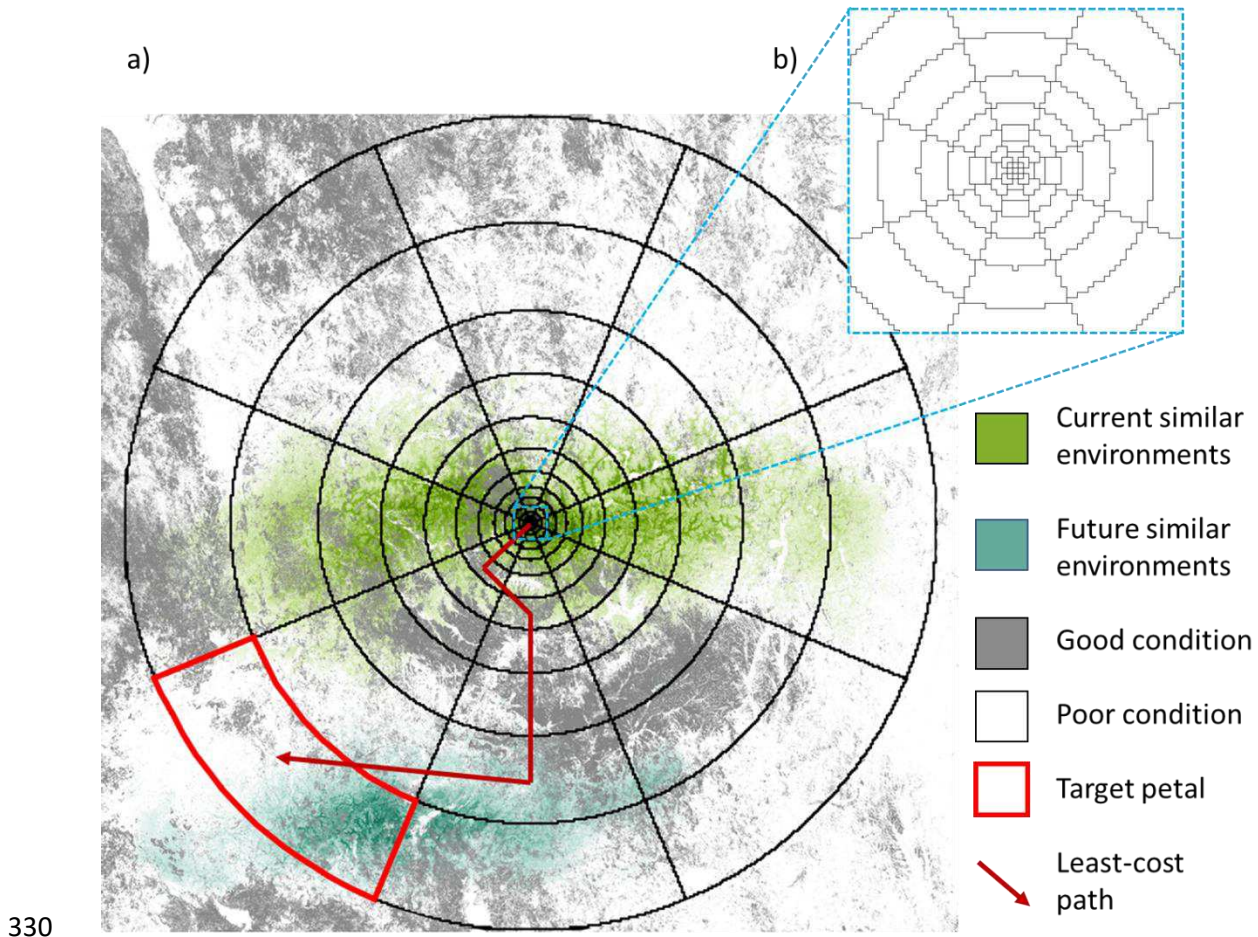


**Fig. 2:** Formalised radial structure as defined in Table S2, with an enlargement of the geometry close to the centre (b) showing the effects of pixelation on radial segments. The larger diagram (a) shows the complete radial structure, with a least-cost path (dark red) connecting the focal cell to a highlighted (red) target segment. More permeable paths span more intact condition. The value of each segment is determined by the ecological similarity of the environment at cells within this segment, relative to the current environment of the focal cell. This similarity is depicted here for current climatic conditions (green) and a single future climate scenario (turquoise).

338

### 339 *Dispersal rates*

340

341 The potential rate of movement of plant populations under climate change will be determined in the  
 342 first instance by the rate of dispersal of seed. Only once a seed germinates and establishes at a new  
 343 location does the dispersal of pollen and the subsequent persistence of a population become relevant.  
 344 Consequently, whilst pollen can move long distances the reproductive viability of individuals is

345 determined largely by seed dispersal. Differences in seed dispersal strategies result in a range of  
 346 median dispersal distances, and this means that the connectivity of the landscape will vary markedly  
 347 for different species. In order to address this, we calculated the Spatial Resilience Index for multiple  
 348 dispersal distances representing a range of plant dispersal rates, and averaged the final index scores  
 349 across this range. Corlett and Westcott (2013) describe annual dispersal rates of up to 1500m year<sup>-1</sup>  
 350 although most species disperse more slowly. Median dispersal distances ( $\lambda$ ) were calculated for a 50-  
 351 year period and four were used: 3.125, 6.25, 12.5 and 25 km, representing annual dispersal rates of  
 352 62.5, 125, 250 and 500 m year<sup>-1</sup>. These were supplied to a negative exponential dispersal kernel  $p =$   
 353  $e^{-d/\lambda}$ , where  $d$  is the habitat-condition weighted path length between locations. Annual  
 354 exponentially-distributed dispersal rates were scaled up to take into account the implications of  
 355 overlapping distributions over time. The exponential distribution defines a two-dimensional  
 356 probability field ( $p^t$ ) around each grid cell  $i$  for a single year's dispersal to other cells  $j$ . The  
 357 probability of dispersal from this original source  $i$  in the following year can then be calculated from  
 358 all cells  $j$  with a probability  $p^t_j$  using the same exponential distribution. A new expanded two-  
 359 dimensional probability field ( $p^{t+1}$ ) is then calculated as the product of each cellwise probability from  
 360 time  $t$  ( $p^t_j$ ) and the exponential distribution. This was explored through simulation for 50 years and, in  
 361 line with the Central Limit Theorem, the resultant probability density functions rapidly converged to a  
 362 Gaussian distribution as  $P = e^{-d^2/\Lambda}$ , where  $\Lambda$  increases linearly with the number of iterations ( $g$ ) as  
 363  $\Lambda = 5.79g$ . The resultant 50-year dispersal kernel can therefore be expressed in terms of the original  
 364 exponential median distance  $\lambda$  as

$$365 \quad P = e^{-\left(\frac{d^2}{5.79g\lambda}\right)}$$

366 To derive habitat-weighted path lengths ( $d$ ) across graph edges between segments, the Euclidian  
 367 distances between the centres of adjacent segments were multiplicatively weighted by the mean  
 368 habitat condition ( $h$ ) of their respective segments inversely scaled between 2.5 ( $h=0$ ) and 1 ( $h=1$ ).  
 369 This results in the traversal of a completely degraded segment ( $h=0$ ) costing 2.5 times that of a  
 370 completely intact petal ( $h=1$ ) of equal size, in line with generic cost factors adopted by Love et al.

371 (2020) and Drielsma et al. (2022). The habitat-weighted length ( $D$ ) of the least cost path from the  
 372 source ( $i$ ) to segment ( $\psi$ ) through multiple segments ( $q$ ) was then calculated as the sum of the habitat-  
 373 weighted lengths across all  $n$  traversed segments as

$$374 \quad D_{i\psi} = \sum_{q=1}^n d_q$$

### 375 *Cellwise calculation*

376

377 The Spatial Resilience Index was calculated for each grid cell ( $i$ ), using the formalised petal  
 378 framework, which was laid over the 9" grid surrounding that cell. The condition ( $h_\psi$ ) of each segment  
 379 ( $\psi$ ) was calculated as a weighted sum of the habitat condition ( $h_j$ ) values of all cells falling within this  
 380 segment, with the contribution of each cell weighted by its pairwise similarity ( $s_{ij}$ ) in predicted species  
 381 composition to the current composition of the focal cell (i.e.  $\sum_{j=1}^n s_{ij} h_j$ ). The least-cost path  
 382 connecting each segment ( $\psi$ ) to the focal cell ( $i$ ) was then determined, and the connectedness ( $\chi$ ),  
 383 given the condition surface being tested, relative to that for an intact condition surface calculated as

384  $\chi_{i\psi} = D_{i\psi} \sum_{j=1}^n s_{ij} h_j$  by estimating the shortest habitat-weighted path distance as described in

385 Drielsma et al. (2007b). Overall connectedness ( $c$ ) of cell  $i$  to all segments under a given scenario  $k$

386 was then calculated as  $c_{ik} = \sum_{\psi=1}^{n\psi} \chi_{i\psi}$

387 For each dispersal distance, the index was derived for all 13 ( $m$ ) climate scenarios (current climate  
 388 and 12 future scenarios) and the Limited Degree of Confidence statistic (Bryan et al. 2014; Ferrier et  
 389 al. 2020; McInerney et al. 2012) applied to provide a robust summary metric of connectedness across  
 390 all scenarios. The subsequent four results were then averaged to provide the cellwise estimate ( $\rho_i$ ) of  
 391 projected connectedness conferred by the surrounding landscape configuration:

$$392 \quad \rho_i = \frac{\sum_{\lambda=1}^{\lambda=4} \left( \frac{\sum_{k=1}^m c_{ik}}{m} + \min\{c_{i1}, \dots, c_{im}\} \right)}{4}$$

393 where  $c_{i0}$  is idealised connectedness of an entirely intact landscape under current climate.

394

## 395 Calculation of Spatial Resilience Index by summary regions

396

397 The global BERI indicator (Ferrier et al. 2020) aggregates the cellwise calculations ( $\rho_i$ ) to country and398 regional scales by taking the arithmetic mean of all cells within a region ( $N_{region}$ ). However, this

399 approach does not account for the effects of beta diversity on the collective persistence of biodiversity

400 at a regional level (i.e. gamma diversity), as outlined in Ferrier et al. (2004). The Spatial Resilience

401 Index addresses this problem by explicitly accounting for varying levels of compositional similarity,

402 through the sharing of species, between grid cells both within and between reporting regions. This is

403 achieved by weighting the averaging of cellwise index values scaling aggregation according to the

404 compositional uniqueness layer, i.e. the inverse of  $(\sum_{j=1}^{j=N_{all}} s_{ij})$ , generated under baseline climatic

405 conditions (Supplementary Figure S2a). This builds on the approach previously described by Ferrier

406 et al. (2004) and Allnutt et al. (2008) for weighting the contribution that individual cells make to

407 regional indices of gamma diversity:

408

$$\rho_{region} = \frac{\sum_{i=1}^{i=N_{region}} \left[ \rho_i / \sum_{j=1}^{j=N_{all}} s_{ij} \right]}{\sum_{i=1}^{i=N_{region}} \left[ 1 / \sum_{j=1}^{j=N_{all}} s_{ij} \right]}$$

409

410 Initial reporting for NSW was conducted using the Interim Biogeographic Regionalisation for

411 Australia (IBRA) bioregions (Department of Sustainability Environment Water Populations and

412 Communities 2012). The analysis was conducted within the NSW State boundary. This reflects both

413 higher confidence in the mapping of habitat condition within NSW and the requirements of state-level

414 reporting. Where parts of a given IBRA bioregion lay outside NSW, these cells were excluded from

415 the analysis, and  $N_{region}$  was therefore defined by the intersection of NSW and a given region.416 However, the contribution of areas outside NSW was taken into account through  $\sum_{j=1}^{j=N_{all}} s_{ij}$ .

417 A further output to aid interpretation was generated in the form of summary histograms for each  
418 region, recording the frequency of the cellwise index in bins of width 0.02. The distribution of values  
419 within a region provides useful information in addition to the single summary statistic.

420

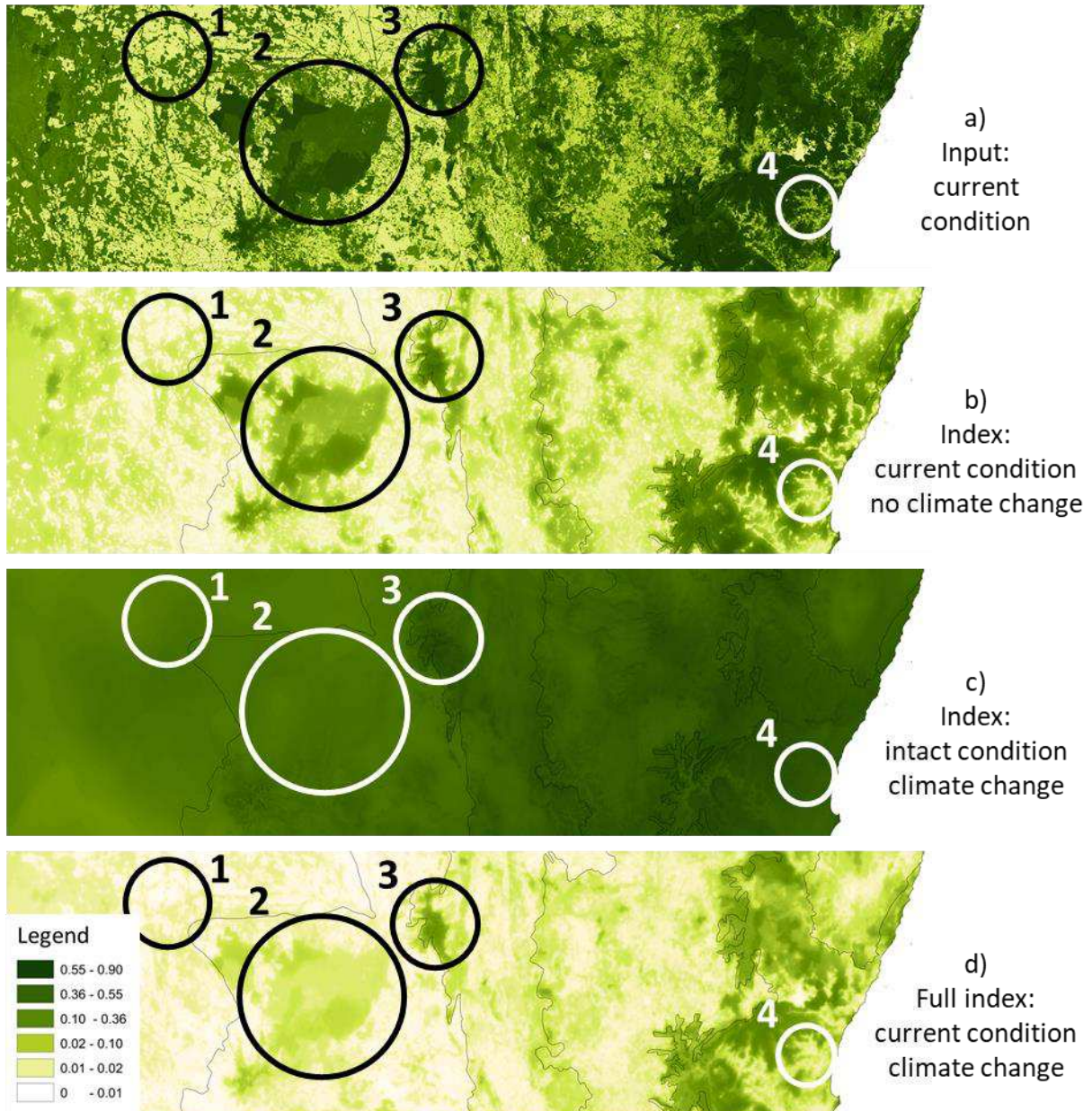
## 421 **Results**

422

423 Key interactions between components shaping cellwise results for the Spatial Resilience Index are  
424 illustrated for a selected portion of NSW in Figure 3. This figure shows how the spatial configuration  
425 of habitat condition (panel a) determines the current connectedness of habitat in the absence of  
426 climate change (panel b), and how this combines with the expected effect of climate velocity under  
427 plausible climate futures (panel c) to shape results for the full index (panel d). Four areas are  
428 highlighted to explore these interactions. Two largely intact areas, the Pilliga Forest (area 2) and  
429 Mount Kaputar National Park (area 3) show how the moderating effects of terrain can enhance the  
430 capacity of landscapes to retain biodiversity under climate change. Despite the Pilliga Forest being a  
431 larger area in good condition, and therefore providing good habitat connectedness under current  
432 climate (Figure 3a and b), its flatter terrain means that climate velocity will be higher for this  
433 landscape (Figure 3c), resulting in lower overall spatial resilience (Figure 3d) than for the complex  
434 dissected terrain of Mount Kaputar which should allow many species to move a relatively short  
435 distance (e.g. upslope) to track shifts in suitable habitat under climate change.

436 A similar situation is demonstrated by the other two landscapes highlighted in Figure 3, where land-  
437 use change has been greater – i.e. Walgett to Lightning Ridge (area 4) and Nambucca River Valley  
438 (area 3). The fragmentation of intact habitats in the Walgett to Lightning Ridge area (Figure 3a and b),  
439 combined with the high climate velocity expected in this flat terrain (Figure 3c), results in very low  
440 spatial resilience (Figure 3d). While habitats in the Nambucca River Valley are also quite fragmented,  
441 the effect this has on spatial resilience is offset, to some extent, by the topographic complexity and  
442 therefore lower climate velocity, of this landscape.

443 State-wide results for the Spatial Resilience Index are presented in Figure 4, both at raw grid-cell  
444 resolution and summarised by Interim Biogeographic Regionalisation for Australia (IBRA)  
445 bioregions (Department of Sustainability Environment Water Populations and Communities 2012).  
446 The patterns highlighted in Figure 3 hold true across the whole state (Figure 4a), with highest spatial  
447 resilience in the topographically buffered and more intact areas near the coast, and reduced resilience  
448 in the more heavily utilised areas, and/or in areas of flatter terrain, and therefore higher climate



449

450 **Fig. 3:** Interaction between components of the Spatial Resilience Index for the area inland from Coffs Harbour  
 451 in northern NSW: a) current habitat condition; b) the Spatial Resilience Index derived using current condition  
 452 but assuming, hypothetically, no future change in climate – this highlights the effect of habitat connectedness on  
 453 spatial resilience; c) the Spatial Resilience Index derived using future climate scenarios but assuming,  
 454 hypothetically, that NSW is covered by intact native habitat – this highlights the effect of climate velocity on  
 455 spatial resilience; and d) the full Spatial Resilience Index combining the effects of both habitat connectedness  
 456 and climate velocity. All four maps share the same colour ramp. Four geographical areas are highlighted: 1. The  
 457 Pilliga Forest, 2. Mount Kaputar National Park, 3. Nambucca River Catchment 4. Walgett to Lightning Ridge.

458

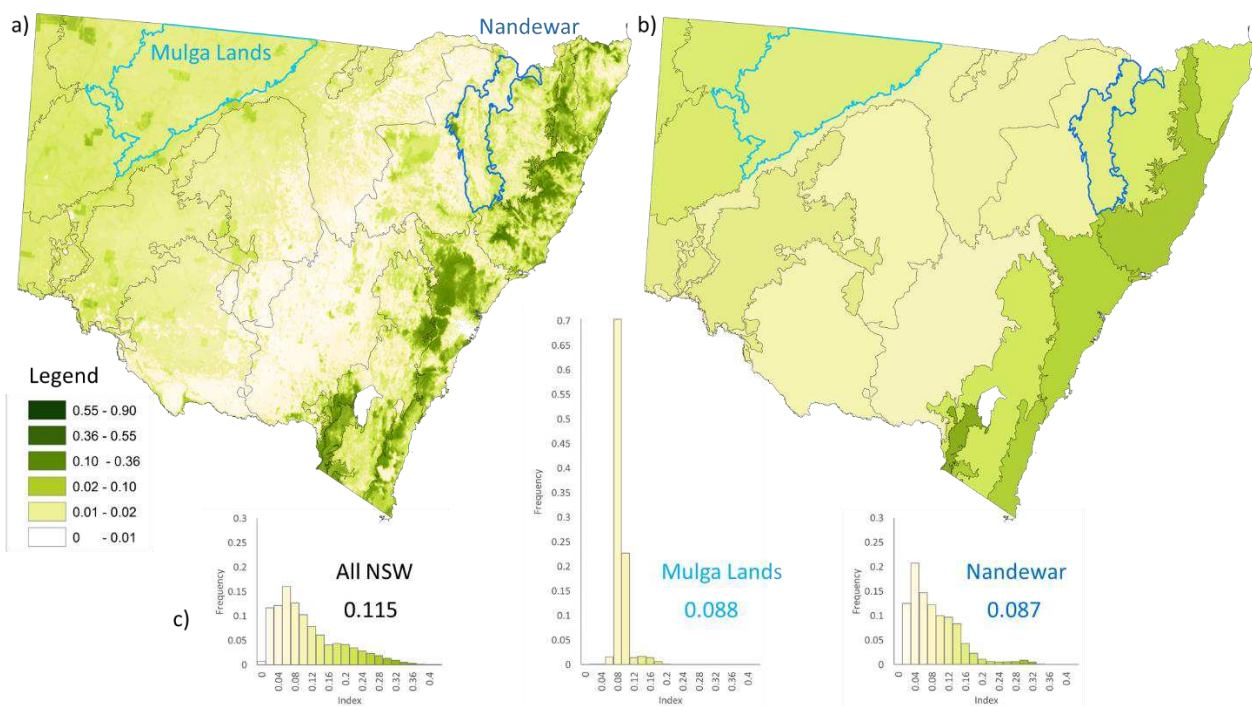
459

460

461 velocity, further inland (i.e. the western two-thirds of the state) even where the habitat of these areas  
 462 remains relatively intact. The mapping of results summarised by IBRA bioregions (Figure 4b) broadly  
 463 reflects the patterns exhibited by the cellwise results. However, it should be noted that most of the  
 464 bioregions near the coast have a lower aggregated score than might be expected. This is because the  
 465 consideration given to beta-diversity patterns, when summarising the index by regions, is accounting  
 466 for compositional differences between the more intact steeper-terrain portions of these regions,  
 467 exhibiting high spatial resilience, and the less intact portions on flatter terrain, exhibiting much lower  
 468 resilience.

469 Individual components of the index, as illustrated in Figure 3, were calculated to aid interpretation of  
 470 the final index. A numerical breakdown of these components by IBRA bioregion is shown in Figure  
 471 5, where the committed impact of projected climate change is separated from the added impact of past  
 472 habitat loss on connectedness, which can potentially be addressed through habitat restoration.

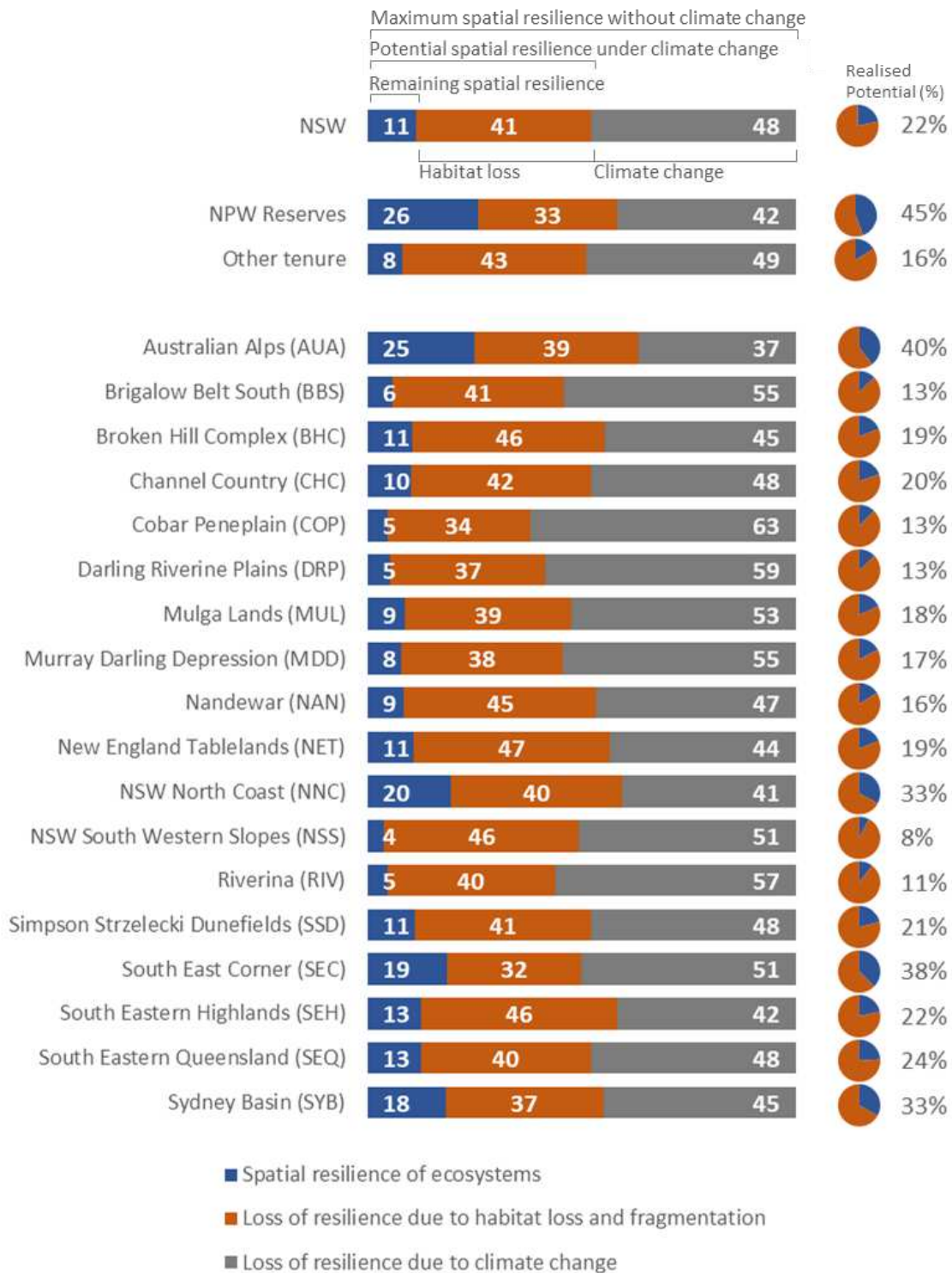
473



474

475 **Fig. 4:** Spatial Resilience Index at raw grid resolution (a), summarised by IBRA region (b) and as frequency  
 476 histograms (c). Two example bioregions are highlighted with similar summary scores for the index, but  
 477 exhibiting very different distributions of scores at the resolution of individual grid-cells.

478



479

480 **Fig. 5:** Breakdown of the Spatial Resilience Index for each reporting unit (IBRA bioregion) in NSW. The final  
 481 index is a product of the combined effects of projected climate change (grey) and habitat loss (orange). The sum  
 482 of the blue and orange bars indicates the maximum level of spatial resilience achievable in the absence of  
 483 climate-change mitigation. The currently realised proportion of this potential is shown in the pie charts to the  
 484 right.

## 485 **Discussion**

486

487

### 488 Advances made in assessing spatial resilience

489

490 Here we have successfully advanced an approach to assessing, at high spatial resolution, the capacity  
491 of landscapes to retain biodiversity in the face of climate change through three major refinements and  
492 extensions of the BERI indicator previously applied at global scale. Firstly, formalisation of the  
493 geometry of the radial grid employed in this approach has enhanced the rigour and consistency with  
494 which the connectedness of habitat close to each focal cell is assessed. Secondly, the incorporation of  
495 multiple dispersal-distance settings has allowed differences in dispersal strategies to be accounted for  
496 more effectively in assessing impacts of habitat connectedness on biodiversity persistence. Thirdly,  
497 incorporation of beta diversity into the aggregation of cellwise results to report the Spatial Resilience  
498 Index at whole-region level has ensured that such reporting better reflects expected changes in the  
499 collective persistence of gamma diversity for any given region, as opposed to a simple average of  
500 local persistence levels within that region.

501

### 502 Caveats and limitations of the approach

503

504 The technique we have used to calculate path lengths across the landscape necessarily assumes that  
505 agents will pass through all segments along the least cost path to the destination. This may be a  
506 reasonable assumption for many animals, but it is worth noting that some dispersal mechanisms  
507 involving, for example, wind-borne propagules or flying vectors may be able to ignore areas of locally  
508 degraded habitat, and dispersal in such cases may be better represented by a simple dispersal kernel  
509 (Shaw et al. 2006). A further implicit assumption is that dispersal distances remain constant across the  
510 whole analysis region, and there is no effect of local landscape heterogeneity on the requirement or  
511 ability of species to disperse.

512 In its current form, the Spatial Resilience Index does not take the environmental suitability of  
513 intervening habitat into account. The permeability of habitat is estimated purely as a function of its  
514 intactness or condition, not as a function of the type of habitat relative to that of the focal cell – e.g. an  
515 intact area of rainforest is assumed to offer the same permeability as an intact area of open woodland,  
516 regardless of whether the focal cell is itself rainforest or woodland. Whilst it would be possible to  
517 address this in the current framework for a static climate, doing so for a changing climate would  
518 require adoption of a more mechanistic approach such as the metacommunity modelling of Mokany et  
519 al. (2012) to fully account for the complex interactions between dispersal rates, available habitat and  
520 environmental suitability.

521 Another critical aspect of dispersal is time. The index is here calculated for a 2070 future, allowing 50  
522 years of dispersal, but could readily be applied to other future periods. Importantly, however,  
523 appropriate kernels for multiple years of dispersal are not simple accumulations of annual dispersal  
524 kernels. The spatio-temporal analysis, and associated equation for multi-year dispersal, developed  
525 here in relation to the negative exponential kernel have potential for broader application in landscape  
526 ecology.

527 The results presented here for NSW are based on a GDM model for vascular plants. While  
528 compositional turnover in plants is well suited to environmental modelling due to a good coupling to  
529 local growing conditions and can be a good surrogate for other biological groups given the role plants  
530 play in defining habitat for other species, there are limitations to this assumption. Many mobile  
531 species will utilise specific landscape features when moving across the landscape, and may therefore  
532 be more affected by changes in the structural, rather than compositional, attributes of vegetation.

533 A final caveat is that the Spatial Resilience Index does not consider the possibility that the  
534 fundamental climatic niche of many species might be broader than that suggested by the currently  
535 realised distribution of the species concerned. Nor does it consider potential for species to undergo  
536 evolutionary adaptation in response to climatic conditions shifting beyond previous limits of tolerance  
537 (Bush et al. 2019).

### 538 Implications of initial results for policy and management

539

540 The results presented in Figure 5 indicate that climate change over the next 50 years is likely to have a  
541 strong effect on the availability and accessibility of habitat in climatic environments similar to those  
542 currently occupied by species throughout NSW. These results suggest that, even if NSW were still  
543 covered entirely by intact native habitat, the State's capacity to retain biodiversity under climate  
544 change would be only 52% of that expected if climatic conditions remained unchanged. In other  
545 words, future climate change alone is responsible for a 48% reduction in spatial resilience. This loss  
546 can be reduced only through global climate-change mitigation and is therefore dependent on factors  
547 largely beyond the control of land-management actions within NSW. Given that the maximum level  
548 of spatial resilience achievable through land-management actions is limited to 52% it makes sense to  
549 assess the need and potential for such actions relative to this constraint. This is the approach adopted  
550 in the pie charts depicted in Figure 5, where the spatial resilience associated with the current condition  
551 and configuration of native habitat across NSW, and within each of the State's bioregions, is  
552 expressed as a percentage of the maximum possible under the climate scenarios analysed here. These  
553 results indicate considerable potential, across all bioregions, to increase capacity to retain biodiversity  
554 under climate change through on-ground actions designed to restore and enhance the area, condition  
555 and connectedness of native habitat.

556

### 557 Extending application of the indicator to prioritising actions

558

559 The results presented in Figure 5 help to highlight regions where the impact of climate change is  
560 likely to be felt more strongly than others, and where most potential exists to ameliorate this impact  
561 through land-management actions. However, it is important not to treat the cellwise results for the  
562 Spatial Resilience Index presented in this paper as a guide to prioritising where best to locate such  
563 actions within any given region. In its raw form, the Spatial Resilience Index for a grid-cell is purely a  
564 measure of the capacity of the surrounding landscape to support biodiversity currently associated with  
565 that cell, in the face of climate change. Considerable potential exists, however, to use the analytical

566 capability established here as a foundation for building analyses aimed at prioritising on-ground  
567 management actions. For example, to assess the relative benefit of restoring habitat within a given  
568 parcel of land, the Spatial Resilience Index would be derived twice – first using the current condition  
569 layer for NSW (as for the results presented here), and then using a modified version of this layer in  
570 which all grid cells within the proposed restoration area are set to best possible condition. The  
571 difference between the two resulting values of the index then provides a measure of the expected  
572 benefit of the proposed action. If this marginal benefit is calculated for each individual grid-cell, in  
573 turn, across NSW then this analysis could be used to generate fine-resolution gridded surfaces  
574 indicating the relative priority for applying a given action across the State, as per the general approach  
575 to priority mapping described by Ferrier and Drielsma (2010).

576

## 577 **Conclusions**

578

579 Development of the Spatial Resilience Index provides a repeatable indicator for measuring the  
580 capacity of landscapes to retain biodiversity under climate change, as a function of the condition and  
581 spatial configuration of native habitat. Initial application of this indicator across NSW using the  
582 biodiversity indicator program's mapping of current habitat condition has revealed considerable  
583 variation in spatial resilience both between and within the State's bioregions. This variation results  
584 largely from the interplay between variation in levels of habitat loss and fragmentation, and variation  
585 in the extent to which climate velocity is likely to be moderated by topographic complexity. However,  
586 considerable potential exists across all regions to improve current levels of spatial resilience through  
587 on-ground actions aimed at restoring or enhancing habitat condition and connectedness. The  
588 analytical capability established by this study now offers a solid foundation for future mapping of  
589 priority areas for action, at fine spatial resolution across the State.

590

591 **Figures**

592

593 **Fig. 1:** Workflow for the calculation of the Spatial Resilience Index.

594 **Fig. 2:** Formalised radial structure as defined in Table S2, with an enlargement of the geometry close to the  
 595 centre (b) showing the effects of pixelation on radial segments. The larger diagram (a) shows the complete  
 596 radial structure, with a least-cost path (dark red) connecting the focal cell to a highlighted (red) target segment.  
 597 More permeable paths span more intact condition. The value of each segment is determined by the ecological  
 598 similarity of the environment at cells within this segment, relative to the current environment of the focal cell.  
 599 This similarity is depicted here for current climatic conditions (green) and a single future climate scenario  
 600 (turquoise).

601 **Fig. 3:** Interaction between components of the Spatial Resilience Index for the area inland from Coffs Harbour  
 602 in northern NSW: a) current habitat condition; b) the Spatial Resilience Index derived using current condition  
 603 but assuming, hypothetically, no future change in climate – this highlights the effect of habitat connectedness on  
 604 spatial resilience; c) the Spatial Resilience Index derived using future climate scenarios but assuming,  
 605 hypothetically, that NSW is covered by intact native habitat – this highlights the effect of climate velocity on  
 606 spatial resilience; and d) the full Spatial Resilience Index combining the effects of both habitat connectedness  
 607 and climate velocity. All four maps share the same colour ramp. Four geographical areas are highlighted: 1. The  
 608 Pilliga Forest, 2. Mount Kaputar National Park, 3. Nambucca River Catchment 4. Walgett to Lightning Ridge.

609 **Fig. 4:** Spatial Resilience Index at raw grid resolution (a), summarised by IBRA region (b) and as frequency  
 610 histograms (c). Two example bioregions are highlighted with similar summary scores for the index, but  
 611 exhibiting very different distributions of scores at the resolution of individual grid-cells.

612 **Fig. 5:** Breakdown of the Spatial Resilience Index for each reporting unit (IBRA bioregion) in NSW. The final  
 613 index is a product of the combined effects of projected climate change (grey) and habitat loss (orange). The sum  
 614 of the blue and orange bars indicates the maximum level of spatial resilience achievable in the absence of  
 615 climate-change mitigation. The currently realised proportion of this potential is shown in the pie charts to the  
 616 right.

617

**618 Declarations**

619

620 Funding: This work was funded by the NSW Environmental Trust.

621 Conflicts of interest/competing interests: The authors have no relevant financial or non-financial  
622 interests to disclose.

623 Ethics approval: Not applicable

624 Consent to participate: Not applicable

625 Consent for publication: Not applicable

626 Availability of data and material: The project drew on input data and models developed prior to these  
627 analyses. NARCLiM climate data can be downloaded from

628 <https://climatedata.environment.nsw.gov.au/>. The datasets generated during the current study are  
629 available from the corresponding author on reasonable request.

630 Code availability: The project used and developed custom code tailored to specific hardware and  
631 existing GDM modelling processes at the two institutions (C++/CUDA; NSW Department of  
632 Planning, Industry and Environment; C++/OpenMP/OpenMPI: CSIRO). Generalised example code  
633 can be obtained from the corresponding author on reasonable request.

634 Author's contributions: All authors contributed to the design of the analyses and the writing of the  
635 manuscript. JL and TH coded and ran the analyses and mapped the results.

636

637

638 **References**

639

- 640 Allnutt TF, Ferrier S, Manion G et al (2008) A method for quantifying biodiversity loss and its application to a  
641 50-year record of deforestation across Madagascar. *Conservation Letters* 1(4):173-181
- 642 Baumgartner JB, Esperon-Rodriguez M, Beaumont LJ (2018) Identifying in situ climate refugia for plant  
643 species. *Ecography* 41(11):1850-1863
- 644 Beier P, Hunter ML, Anderson M (2015) Conserving Nature's Stage. *Conservation Biology* 29(3):613-617
- 645 Blois JL, Williams JW, Fitzpatrick MC, Jackson ST, Ferrier S (2013) Space can substitute for time in predicting  
646 climate-change effects on biodiversity. *Proc. Natl. Acad. Sci. U. S. A.* 110(23):9374-9379
- 647 Brito-Morales I, Garcia Molinos J, Schoeman DS et al (2018) Climate Velocity Can Inform Conservation in a  
648 Warming World. *Trends in ecology & evolution* 33(6):441-457
- 649 Bryan BA, Nolan M, Harwood TD et al (2014) Supply of carbon sequestration and biodiversity services from  
650 Australia's agricultural land under global change. *Global Environmental Change* 28(0):166-181
- 651 Bush A, Catullo R, Mokany K, Harwood T, Hoskins AJ, Ferrier S (2019) Incorporating existing thermal  
652 tolerance into projections of compositional turnover under climate change. *Global Ecology and Biogeography*  
653 28(6):851-861
- 654 Carroll C, Roberts DR, Michalak JL et al (2017) Scale-dependent complementarity of climatic velocity and  
655 environmental diversity for identifying priority areas for conservation under climate change. *Glob. Change Biol.*  
656 23(11):4508-4520
- 657 Corlett RT, Westcott DA (2013) Will plant movements keep up with climate change? *Trends in Ecology &*  
658 *Evolution* 28(8):482-488
- 659 Cumming GS (2011) Spatial resilience: integrating landscape ecology, resilience, and sustainability. *Landscape*  
660 *Ecology* 26(7):899-909
- 661 Department of Sustainability Environment Water Populations and Communities (2012) Interim Biogeographic  
662 Regionalisation for Australia (IBRA), Version 7 (Bioregions and Subregions) Australian Government  
663 Department of Sustainability, Environment, Water, Population and Communities Canberra, Australia, pp. 2
- 664 Donaldson L, Wilson RJ, Maclean IMD (2017) Old concepts, new challenges: adapting landscape-scale  
665 conservation to the twenty-first century. *Biodivers. Conserv.* 26(3):527-552
- 666 Drielsma M, Ferrier S, Manion G (2007a) A raster-based technique for analysing habitat configuration: The  
667 cost-benefit approach. *Ecological Modelling* 202(3-4):324-332
- 668 Drielsma M, Ferrier S, Manion G (2007b) A raster-based technique for analysing habitat configuration: The  
669 cost-benefit approach. *Ecological Modelling* 202(3):324-332
- 670 Drielsma M, Love J, White M, Williams K, Ferrier F (2020) A model-based indicator of capacity for  
671 biodiversity persistence using vascular plant records and habitat condition, Biodiversity Indicator Program  
672 Implementation Report. . Department of Planning, Industry and Environment NSW, Sydney, Australia: ,
- 673 Drielsma M, Manion G, Love J, Williams K, Harwood T, Saremi H (2015) 3C modelling for biodiversity under  
674 climate change
- 675 Drielsma MJ, Love J, Taylor S, Thapa R, Williams KJ (2022) General Landscape Connectivity Model (GLCM):  
676 a new way to map whole of landscape biodiversity functional connectivity for operational planning and  
677 reporting. *Ecological Modelling* 465:109858
- 678 Drielsma MJ, Love J, Williams KJ et al (2017) Bridging the gap between climate science and regional-scale  
679 biodiversity conservation in south-eastern Australia. *Ecological Modelling* 360:343-362
- 680 Ferrier S, Drielsma M (2010) Synthesis of pattern and process in biodiversity conservation assessment: a  
681 flexible whole-landscape modelling framework. *Diversity and Distributions* 16(3):386-402

- 682 Ferrier S, Harwood TD, Ware C, Hoskins AJ (2020) A globally applicable indicator of the capacity of terrestrial  
683 ecosystems to retain biological diversity under climate change: The bioclimatic ecosystem resilience index.  
684 *Ecological Indicators* 117:106554
- 685 Ferrier S, Harwood TD, Williams KJ (2012) Using generalised dissimilarity modelling to assess potential  
686 impacts of climate change on biodiversity composition in Australia, and on the representativeness of the  
687 National Reserve System. CSIRO, Canberra. [https://research.csiro.au/climate/wp-](https://research.csiro.au/climate/wp-content/uploads/sites/54/2016/03/13E_CAF-Working-Paper-13E.pdf)  
688 [content/uploads/sites/54/2016/03/13E\\_CAF-Working-Paper-13E.pdf](https://research.csiro.au/climate/wp-content/uploads/sites/54/2016/03/13E_CAF-Working-Paper-13E.pdf),
- 689 Ferrier S, Manion G, Elith J, Richardson K (2007) Using generalized dissimilarity modelling to analyse and  
690 predict patterns of beta diversity in regional biodiversity assessment. *Diversity and Distributions* 13(3):252-264
- 691 Ferrier S, Powell GV, Richardson KS et al (2004) Mapping more of terrestrial biodiversity for global  
692 conservation assessment. *BioScience* 54(12):1101-1109
- 693 Fitzpatrick MC, Sanders NJ, Ferrier S, Longino JT, Weiser MD, Dunn R (2011) Forecasting the future of  
694 biodiversity: a test of single- and multi-species models for ants in North America. *Ecography* 34(5):836-847
- 695 Gillson L, Dawson TP, Jack S, McGeoch MA (2013) Accommodating climate change contingencies in  
696 conservation strategy. *Trends in Ecology & Evolution* 28(3):135-142
- 697 Hannah L, Midgley G, Andelman S et al (2007) Protected area needs in a changing climate. *Frontiers in*  
698 *Ecology and the Environment* 5(3):131-138
- 699 Holling CS (1973) Resilience and stability of ecological systems. *Annual Review of Ecology and Systematics*  
700 4:1-23
- 701 Hutchinson M, Xu T (2015) Methodology for generating Australia-wide surfaces and associated grids for  
702 monthly mean daily maximum and minimum temperature, rainfall, pan evaporation and solar radiation for the  
703 periods 1990–2009, 2020–2039, 2060–2079. Report to the NSW Office of Environment and Heritage, 7  
704 September 2015. Australian National University,
- 705 Jones KR, Watson JEM, Possingham HP, Klein CJ (2016) Incorporating climate change into spatial  
706 conservation prioritisation: A review. *Biological Conservation* 194:121-130
- 707 Keeley ATH, Ackerly DD, Cameron DR et al (2018) New concepts, models, and assessments of climate-wise  
708 connectivity. *Environmental Research Letters* 13(7)
- 709 Love J, Drielsma M, Williams K, Thapa R (2020) Integrated model–data fusion approach to measuring habitat  
710 condition for ecological integrity reporting: Implementation for habitat condition indicators, Biodiversity  
711 Indicator Program, Implementation Report. Department of Planning, Industry and Environment NSW, Sydney,  
712 Australia: ,
- 713 McInerney D, Lempert R, Keller K (2012) What are robust strategies in the face of uncertain climate threshold  
714 responses? *Climatic Change* 112(3):547-568
- 715 Mokany K, Harwood TD, Ferrier S (2013) Comparing habitat configuration strategies for retaining biodiversity  
716 under climate change. *Journal of Applied Ecology* 50(2):519-527
- 717 Mokany K, Harwood TD, Williams KJ, Ferrier S (2012) Dynamic macroecology and the future for biodiversity.  
718 *Global Change Biology* 18(10):3149–3159
- 719 Nunez TA, Lawler JJ, Mcrae BH et al (2013) Connectivity Planning to Address Climate Change. *Conservation*  
720 *Biology* 27(2):407-416
- 721 Prober SM, Doerr VAJ, Broadhurst LM, Williams KJ, Dickson F (2019) Shifting the conservation paradigm: a  
722 synthesis of options for renovating nature under climate change. *Ecol. Monogr.* 89(1)
- 723 Quinlan AE, Berbes-Blazquez M, Haider LJ, Peterson GD (2016) Measuring and assessing resilience:  
724 broadening understanding through multiple disciplinary perspectives. *Journal of Applied Ecology* 53(3):677-687
- 725 Shaw MW, Harwood TD, Wilkinson MJ, Elliott L (2006) Assembling spatially explicit landscape models of  
726 pollen and spore dispersal by wind for risk assessment. *Proceedings of the Royal Society B: Biological Sciences*  
727 273(1594):1705-1713

- 728 Stein BA, Staudt A, Cross MS et al (2013) Preparing for and managing change: climate adaptation for  
729 biodiversity and ecosystems. *Frontiers in Ecology and the Environment* 11(9):502-510
- 730 Urban MC, Bocedi G, Hendry AP et al (2016) Improving the forecast for biodiversity under climate change.  
731 *Science* 353(6304):1113-+
- 732 van Kerkhoff L, Munera C, Dudley N et al (2019) Towards future-oriented conservation: Managing protected  
733 areas in an era of climate change. *Ambio* 48(7):699-713
- 734

## Supplementary Files

This is a list of supplementary files associated with this preprint. Click to download.

- [HarwoodetalStayingConnectedSupplementary.pdf](#)